IL NUOVO CIMENTO **41 C** (2018) 159
DOI 10.1393/ncc/i2018-18159-7

COLLOQUIA: LaThuile 2018

Measurement of the $t\bar{t}\gamma$ production cross section in proton-proton collisions at $\sqrt{s} = 8$ TeV with the ATLAS detector

J.W. SMITH on behalf of the ATLAS COLLABORATION

II. Physikalisches Institut, Georg-August-Universität - Göttingen, Germany

received 6 September 2018

Summary. — The large centre-of-mass energy available at the Large Hadron Collider allows for the copious production of top quark pairs in association with other final state particles at high transverse momenta. The ATLAS experiment measures the cross-section of top quark pair production in association with a photon at 8 TeV. The results are presented for the cross section measurement in a fiducial region and differentially as a function of the transverse momentum and pseudorapidity of the photon.

1. – Introduction

Top quark pair production in association with a photon ($t\bar{t}\gamma$) plays an important role in testing the Standard Model (SM). It provides a probe into the $t\gamma$ vertex, and thus the electromagnetic coupling.

A photon can originate from the top quark as shown in fig. 1(a). An irreducible background is from photons radiated from initial state partons (fig. 1(b)), however at the LHC this production mechanism is suppressed in favour of gluon-gluon production. A photon can also be radiated from the top quark decay products such as the W boson (fig. 1(c)) or the b-quark (fig. 1(d)). Event selections try to enhance photons that originate from the top quarks and remove those from top quark decay products. Data-driven techniques are used to estimate the main backgrounds. A maximum-likelihood fit is then performed to the templates to extract the fiducial cross section. Differential cross-sections for the transverse momentum (p_T) and the pseudorapidity (η) of the photon are then measured using the same fiducial phase-space.

This analysis [1] is performed using data recorded at $\sqrt{s} = 8$ TeV with the ATLAS [2] detector. A total of 20.2 fb^{-1} is used with only the single lepton final states considered.

© CERN on behalf of the ATLAS Collaboration
Creative Commons Attribution 4.0 License (http://creativecommons.org/licenses/by/4.0)

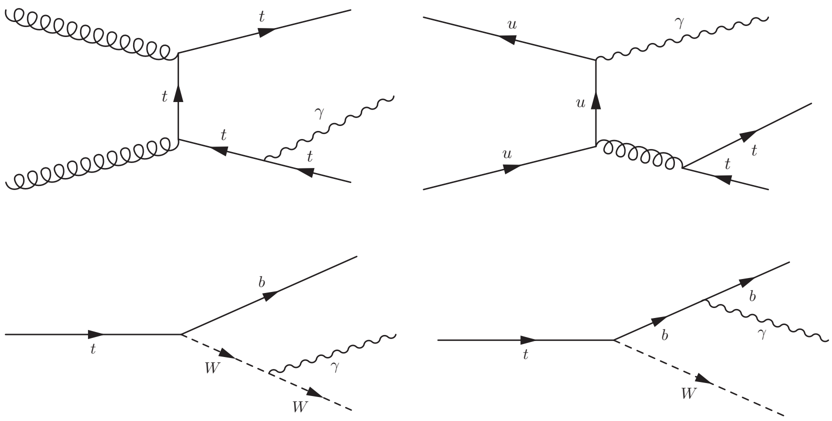

Fig. 1. – Feynman diagrams for example processes that involve top-quark pair production in association with a photon.

2. – Signal and background selections

Selected events are required to have exactly one electron or muon with transverse momentum (p_T) > 25 GeV, as well as one photon with $p_T > 15$ GeV and pseudorapidity ($|\eta|$) < 2.37. At least four jets are required in which at least one should be tagged as a *b-jet* at a 70% working point efficiency. An event is required to have a minimum missing transverse energy (E_T^{miss}) > 30 GeV for the electron channel and > 20 GeV for the muon channel. In the electron channel a cut on the transverse mass of the W boson ($m_T(W)$) is required to be greater than 30 GeV, while in the muon channel $E_T^{miss}+m_T(W) > 60$ GeV. A ΔR cut([1]) between the jet and the photon is required to be > 0.5. This cut reduces photon radiation from quarks. A ΔR cut between the lepton and the photon is placed at > 0.7. This reduces the prompt photon background contributions from top-quark decay products. Finally, for the electron channel the invariant mass of the electron and photon ($m(\gamma, e)$) needs to be outside a 5 GeV mass window around the Z boson mass. This suppresses events originating from $Z+$jets in which an electron is misidentified as a photon.

A fiducial region is defined in which the same cuts as above are used with the exception that cuts on E_T^{miss}, $m_T(W)$ and $m(\gamma, e)$ are removed. This creates a common fiducial region for the electron and muon channel where an "inclusive" and differential fit in this phase space can be performed.

The largest background contribution comes from hadrons, or photons from hadron decays that are misidentified as prompt photons. These are called *hadronic fakes* from hereon. This background originates predominantly from the $t\bar{t}$ process. A template is derived from a hadronic fake enriched control region where a photon fails an identification criteria. The prompt photon contamination in this control region is taken into account and used as a systematic uncertainty.

The second largest background contribution arises from electrons misidentified as photons, called $e \to \gamma$ *fakes* from hereon. These predominantly originate from the dilepton

---

([1]) $\Delta R = \sqrt{(\Delta\eta)^2 + (\Delta\phi)^2}$ describes a cone of radius ΔR in the η-ϕ plane.

final state (specifically in the ee and $e\mu$ channels). Their contribution is estimated from two control regions where one is enriched with $Z \to e^+e^-$ events while the other is enriched with $Z \to e^+ +$ fake γ events. Fake rates are calculated as the ratio of events in these two regions and applied to a modified signal region where a photon is replaced by the electron.

Processes in which a prompt photon is present but not radiated from a top quark form another class of background. These include $W/Z + \text{jets} + \gamma$, single top $+\ \gamma$ and diboson production and are modelled with simulations. A multi-jet background in which a lepton is misidentified as one of the jets also contributes to this background. A control sample with looser lepton identification is used to estimate this contribution.

Figure 2 shows the transverse momentum and pseudorapidity of the photon for signal and all background sources that pass the event selections. The prediction for signal has been normalised to the next-to-leading-order (NLO) calculation. The figures are separated into the electron and muon channel contributions.

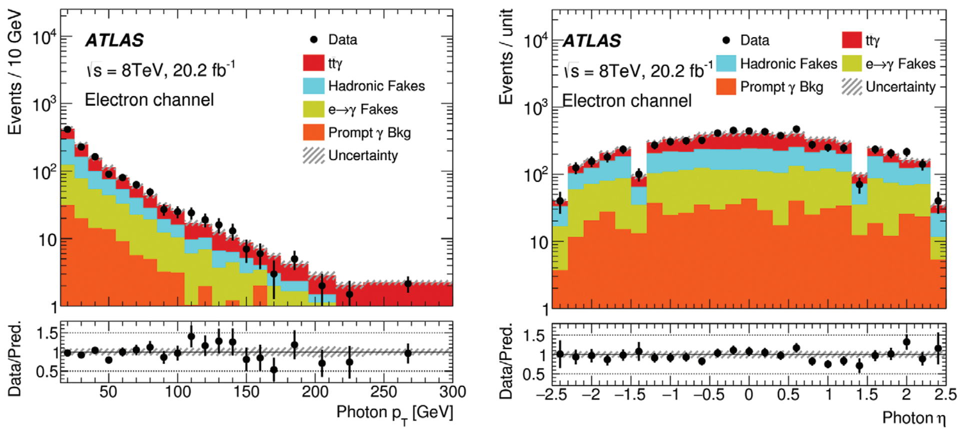

(a)

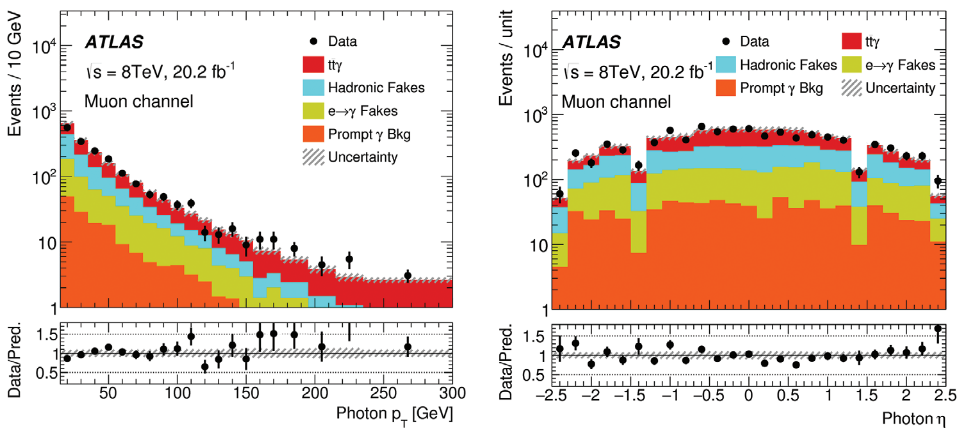

(b)

Fig. 2. – The comparison of data and events passing the selections for the (a) electron and (b) muon channel. The uncertainty band includes statistical and all systematic uncertainties [1].

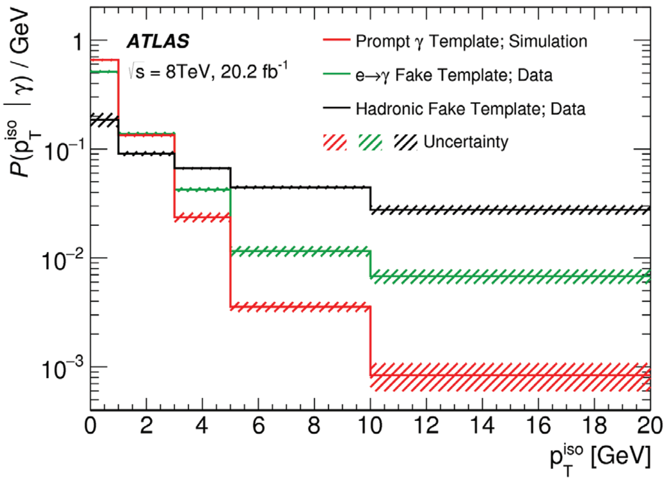

Fig. 3. – The three contributions to the isolation template for the combined electron and muon channels [1].

3. – Analysis strategy

From the definitions of the signal and backgrounds discussed in the previous section, a template consisting of three main categories can be built: prompt photons, hadronic-fakes, and $e \to \gamma$ fakes. The photon track isolation (p_T^{iso}) properties are exploited in these three processes. This is defined as the sum of the transverse momenta of all tracks within a cone of 0.2 rad around the photon. For hadronic and $e \to \gamma$ fakes there are more events in the tail due to increased particle activity closer to the photon. This is shown in fig. 3.

From these templates fiducial and differential cross sections are extracted using a likelihood-fit defined as

$$\mathcal{L} = \prod_{i,j} P(N_{i,j}|N^s_{i,j} + \sum_b N^b_{i,j}) \times \prod_t G(\vartheta|\theta_t, 1). \tag{1}$$

The first product consists of a Poisson function that models the event yield in bin j of the isolation distribution of bin i of the p_T or η distributions. If $i = 1$ a fiducial fit is performed. $N_{i,j}$ is the observed number of data events. $N^s_{i,j}$ is the predicted number of signal events and $\sum_b N^b_{i,j}$ is the total predicted background. This is multiplied by a second product which consists of a Gaussian function of unit width. This models the systematic, t, for a given parametrisation of the uncertainty, θ_t. Importantly, the hadronic fake background enters the fit as a free parameter.

The cross sections are related to $N^s_{i,j}$ by

$$L \times \sigma_i \times C_i \times f_{i,j} = N^s_{i,j}, \tag{2}$$

where for each bin i falling into bin j of the isolation distribution: L is the integrated luminosity, σ_i is the differential or fiducial cross section, C_i is the ratio of the reconstructed events to the generated events in the fiducial region and $f_{i,j}$ is the fraction of events. In

TABLE I. – *The sources of uncertainty and their relative impact on the fiducial cross section* [1].

Source	Relative uncertainty [%]
Hadron-fake tempate	6.3
$e \to \gamma$ fake	6.3
Jet energy scale	4.9
$W\gamma$ + jets	4.0
$Z\gamma$ + jets	2.8
Initial- and final-state radiation	2.2
Luminosity	2.1
Photons	1.4
Single top+γ	1.2
Muon	1.2
Electron	1.0
Scale uncertainty	0.6
Parton shower	0.6
Statistical uncertainty	5.1
Total uncertainty	13

the case of the fiducial cross section, C is essentially the correction factor between the event selection efficiency and the fiducial region efficiency, whereas for the differential measurement it corrects for the migration of events into different bins, i. Thus, for the differential cross-section measurement a bin-by-bin unfolding to particle-level is used.

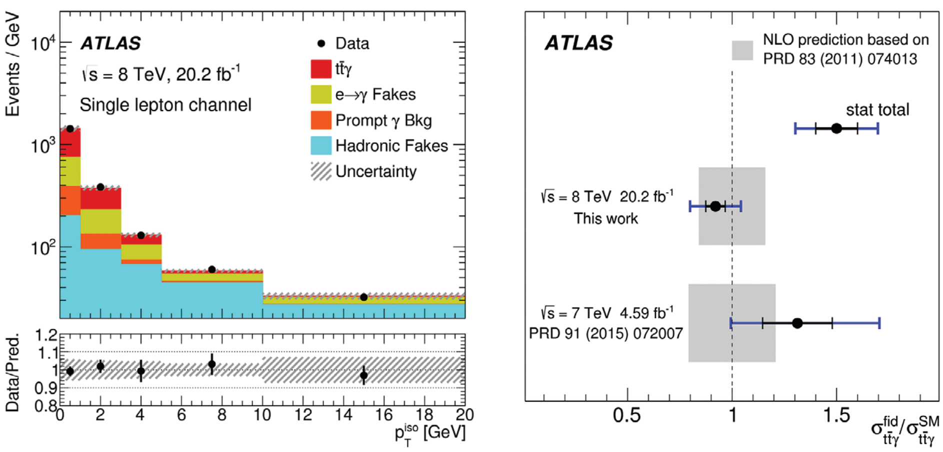

(a) (b)

Fig. 4. – (a) Post-fit isolation distribution for fiducial cross section measurement. (b) The value of μ for the 7 and 8 TeV analyses compared the the theoretical NLO prediction [4]. The vertical line at 1 represents our best understanding of the SM [1].

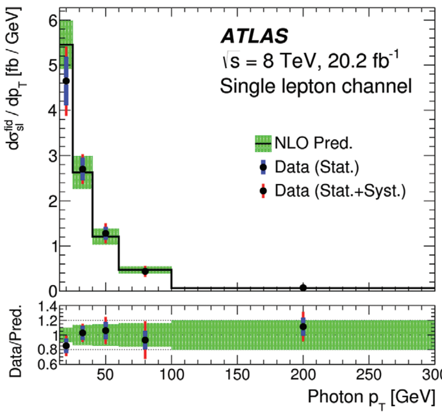

(a)

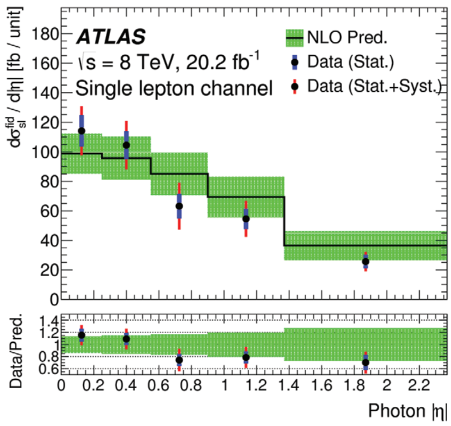

(b)

Fig. 5. – The measured differential cross sections for the (a) p_T and (b) η of the photon in the single lepton channel compared to their theoretical predictions [1].

4. – Results

A maximum-likelihood fit to the template shown in fig. 3 extracts a fiducial cross-section in the single lepton channel of

$$\sigma_{\mathrm{SL}}^{\mathrm{fid}} = 139 \pm 7(\mathrm{stat.}) \pm 17(\mathrm{syst.})\ \mathrm{fb} = 139 \pm 18\ \mathrm{fb}. \tag{3}$$

The dominant uncertainties are shown in table I (relative to the fiducial cross section). The largest contributions come from template related systematics, specifically the hadronic fake and $e \to \gamma$ fake template modelling. The hadronic fake uncertainty is dominated by the prompt photon contamination when deriving the template, whereas the $e \to \gamma$ fake dominant uncertainty arises from varying the $E_{\mathrm{T}}^{\mathrm{miss}}$ requirement in the event selection.

Figure 4(a) shows the post-fit isolation distribution from which 3072 data candidates are extracted. Statistical and systematic uncertainties are included in the error band. Figure 4(b) gives an overview of the fitted μ values for this and the previous work at $\sqrt{s}$ = 7 TeV [3] compared to the SM. The grey shaded area indicates the theoretical NLO prediction [4]. Both results agree with the SM within uncertainties.

Finally, figs. 5(a) and 5(b) show the differential cross sections for the transverse momentum and pseudorapidity of the photon, each with 5 bins. Within uncertainties, all measurements agree with theoretical predictions.

REFERENCES

[1] ATLAS Collaboration, *JHEP*, **11** (2017) 086.
[2] ATLAS Collaboration, *JINST*, **3** (2008) S08003.
[3] ATLAS Collaboration, *Phys. Rev. D*, **91** (2015) 072007.
[4] Melnikov K., Schulze M. and Scharf A., *Phys. Rev. D*, **83** (2011) 074013.